RAA 2021 Vol. **21** No. **7**, 175(10pp) doi:10.1088/1674-4527/21/7/175

http://www.raa-journal.org *http://iopscience.iop.org/raa*

***R**esearch in*
***A**stronomy and*
***A**strophysics*

The research objectives and observational possibilities for fast moving near-Earth asteroids

Anton Pomazan[1,2], Zheng-Hong Tang[1], Nadiia Maigurova[3], Kai Tang[1], Yong Yu[1] and Yin-Dun Mao[1]

[1] Shanghai Astronomical Observatory, Chinese Academy of Sciences, Shanghai 200030, China; *antpomaz@shao.ac.cn*
[2] University of Chinese Academy of Sciences, Beijing 100049, China
[3] Research Institute "Mykolaiv Astronomical Observatory", Mykolaiv 54030, Ukraine

Received 2020 December 15; accepted 2021 March 3

Abstract The paper describes observations of fast-moving near-Earth asteroids (NEAs) made with the small ground-based telescopes of National Time Service Center of Chinese Academy of Science (NTSC of CAS) and Research Institute "Mykolaiv Astronomical Observatory" (RI MAO) by the rotating-drift-scan CCD (RDS CCD) technique. This technique is used to obtain the point images of both the studied objects and reference stars. The results of ongoing follow-up observations of NEAs are discussed. The residual differences ($O-C$) between the observed and calculated positions from JPL ephemeris were generally small for these asteroids. The standard deviations of these differences were typically $\pm(0.2''-0.3'')$ in both coordinates for objects with apparent velocity which substantially exceed FWHM for the given exposure time. The results of comparative statistics for such observations from the MPC database show that this is a good level of precision for NEAs. Moreover, the telescopes with the RDS CCD technique implemented can observe the NEAs that closely approach the Earth and with enough observations can improve the precision of determining their orbital elements and impact predictions.

Key words: astronomical databases: miscellaneous — surveys — methods: observational — techniques: miscellaneous — astrometry — minor planets, asteroids: general

1 INTRODUCTION

Ground-based optical positional observations of Solar System bodies are the basis for the creation of motion theories, defining and clarifying the orbital elements and dynamical parameters. Regular observations of near-Earth objects (NEOs) are one of the most important aspects involved in studying the problem of asteroid-cometary hazard and allow us to refine their orbits. Such research enables predicting a collision of such body with the Earth in the future and taking appropriate measures in advance. Therefore, it becomes critically important to perform efficient follow-up observations. Nowadays, many scientific projects, which are allocated significant funding, are engaged in monitoring known NEOs and the search for new ones. According to current information presented on the International Astronomical Union (IAU) Minor Planet Center[1] (MPC) website, more than 22 000 NEAs are known, including more than 900 NEAs larger than 1 km in diameter. Recent investigations into size-frequency distribution (SFD) and estimations of the completion versus size of NEAs indicate almost full completion, from 990 (Harris & D'Abramo 2015) to 920 (Tricarico 2017) NEAs with sizes 1+km (which is considered equivalent to an absolute magnitude H equal to or brighter than 17.75 mag at a nominal average geometric albedo $pV = 0.14$). At the same time, completion significantly decreases for lower sizes. The total amount of small NEAs in simulations has been estimated as $(7 \pm 2) \times 10^4$ NEAs (Tricarico 2017) larger than 100 m (corresponding to absolute magnitude $H < 22.75$ mag), or 3.5×10^6 (Trilling et al. 2017) for objects with $H \leq 27.3$ mag (around 10 m) and higher orders for smaller sizes.

Currently, there are quite a few asteroid surveys that work in the optical range. Among them are such surveys as the Catalina Sky Survey (CSS) (Larson et al. 1998), Pan-STARRS (Wainscoat et al. 2018), the restarted *NEOWISE* mission (Mainzer et al. 2014) (infrared space-based survey) and ATLAS (Tonry et al. 2018), which account for the bulk of the discoveries of new asteroids

[1]IAU MPC Database. Available online at: https://www.minorplanetcenter.net

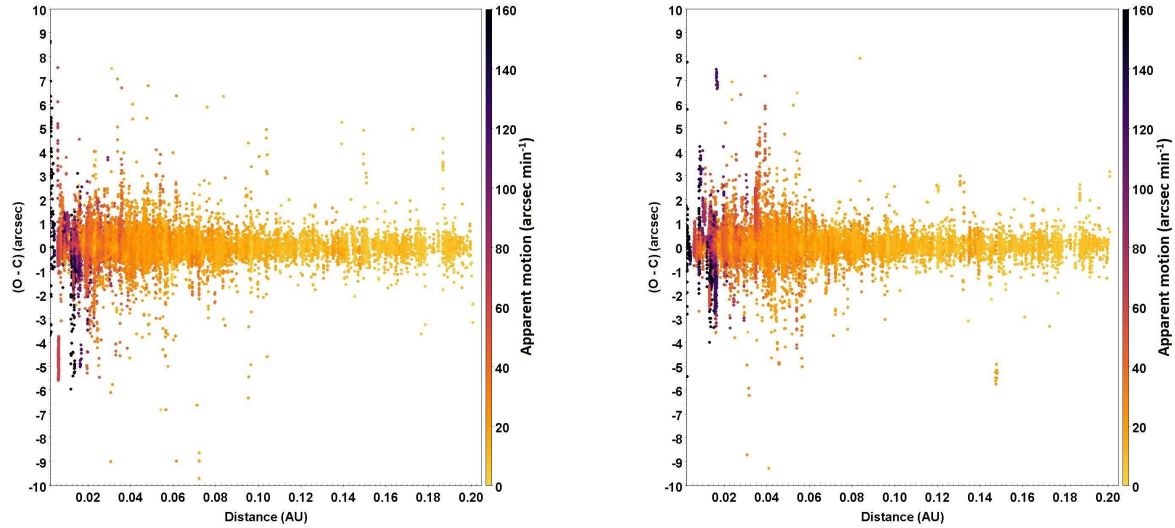

Fig. 1 Distribution of differences $O-C$ in right ascension (*left*) and declination (*right*) versus distances to Earth for PHA observations taken within the range ± 3 d to CA time.

according to data in Jedicke et al. (2015). The number of newly discovered objects grows each year[2]. But despite the efforts being made in this direction, the task of detection of all potential threats cannot be considered solved. The current amount of known small-sized NEAs is significantly larger than the population estimated in simulations (Tricarico 2017; Trilling et al. 2017). The major expectations are associated with the Large Synoptic Survey Telescope (LSST) (Jones et al. 2018) in discovering and achieving the most completeness of NEOs and potentially hazardous asteroids (PHAs) populations.

The population of NEAs includes more than 2000 PHAs for the Earth. Their minimum orbit intersection distance (MOID) is less than or equal to 0.05 AU and diameters are more than 140 m (corresponding to absolute magnitude $H < 22$ mag) which mean they could result in significant consequences and threat to life on Earth. Therefore, it is critically important to detect, identify and systematically monitor such objects to determine the orbital elements with precision sufficient to predict the probability of terrestrial impact as part of Space Situational Awareness. As described in Maigurova et al. (2018), more than 40% of known PHAs were discovered after they had approached a minimum distance to the Earth.

Close approaches (CA) to the Earth by NEAs are the most favorable time for the searching for small-scale objects because at another time they have rather weak apparent magnitudes and require large-diameter telescopes for specific observations. At the same time, their apparent velocity increases significantly which decreases precision of positional observations. All current observations of PHAs since 2010 presented in the IAU MPC database (2020 March) with additional information from JPL's HORIZONS ephemeris system[3] were analyzed regarding apparent motion. The apparent motion has been calculated as the square root of sum of squares of the angular rates of change in apparent right ascension and declination which are taken from JPL's HORIZONS ephemeris calculated at a specified moment in time. Extracted observations have been linked with 1494 known CAs at a distance less than 0.2 AU from the Earth for 1061 PHAs taken from CNEOS. Observations within the range ± 3 d to the moment of known CA were further analyzed. Figure 1 displays the distribution of $(O-C)$ differences in PHA positions for such linked observations versus distance from the Earth in right ascension and declination. The $(O-C)$ differences here mean residuals between observed (O) and ephemeris (C) positions of the objects. The plot shows strong dispersion and increasing standard deviation values of $(O-C)$ differences for the observations with decreasing distance to the Earth and increasing apparent motion of the objects. This, respectively, indicates the difficulty in acquiring observations of such objects. The mean apparent motion is $39''$ min^{-1} (15.6 deg d^{-1}) for observations at distances less than 0.06 AU from the Earth, and at the same time, this part includes around 60% of observations. It should be noticed that there are only a few observations for five PHAs ((503941) 2003 UV11, (357439) 2004 BL86, (308635) 2005 YU55, 2014 JO25, 2015 TB145) with apparent motion more than $160''$ min^{-1} (64 deg d^{-1}) taken during specific international observational campaigns.

[2]Data from JPL Center for NEO Studies (CNEOS), https://cneos.jpl.nasa.gov/stats/

[3]JPL HORIZONS online solar system data and ephemeris computation service, https://ssd.jpl.nasa.gov/?horizons

Table 1 Telescopes' Technical Characteristics

Telescope	Lishan telescope (NTSC)	KT-50 telescope (RI MAO)
Location	China, Lishan mountain	Ukraine, Mykolaiv
Coordinates (IAU MPC):		
Longitude (°E)	109.213	31.970
Latitude (°N)	34.353	46.972
Altitude (m)	950	50
Diameter and type (m)	0.50 Cassegrain	0.50 Maksutov
Focal length (m)	3445	3000
FWHM ($''$)	2.3	2.5
CCD	Alta U9000	
Size (px)	3056×3056	
Pixel size (μm)	12×12	
Scale ($''$ px^{-1})	0.72	0.83
FOV ($'$)	36.7×36.7	42.5×42.5
Filter	without	Johnson V (since 2018)
Exposure (s)		
Reference stars	10 – 15	10
Asteroids	25 – 100 for objects 14.5 – 17.0 mag	60 - 150 for objects 12 – 17.5 mag

Most observations stop at high apparent motion due to difficulties with tracking the object in the field of view (FOV) of the telescope. Strong apparent motion can cause effects of trailing losses, which will bring about a decrease in new discoveries (Tricarico 2017). High speed of visible movement is one of the significant factors (Vereš et al. 2018), which leads to the fact that some of the new discoveries of NEAs remain unconfirmed and may be lost.

This article presents one of the methods for conducting reliable and effective observations of NEAs at the moment of CA to Earth, which was conducted on the telescope of the Lishan Observing Station (National Time Service Center of Chinese Academy of Sciences, NTSC of CAS, China) and the KT-50 telescope (RI MAO, Ukraine). The main feature of the rotating-drift-scan CCD (RDS CCD) technique is usage of a rotational platform and drift scan mode of CCD to obtain separate images of reference stars and objects for the positional observations of celestial bodies with high visible velocities. The application of this combined observational method allows us to get all celestial objects' images as a point, which in turn can be utilized to determine the coordinates of all image centers with sufficient precision.

Section 2 of this paper describes the RDS CCD technique and telescopes where it has been implemented; Section 3 presents obtained NEA observations and astrometric reductions; and in Section 4 positional precision with the RDS CCD method is discussed in terms of comparative statistics with other data from the IAU MPC database.

2 ROTATING-DRIFT-SCAN CCD TECHNIQUE AND TELESCOPES

As was mentioned above, high apparent motion of an object for required exposure time in FOV of a telescope at CA to the Earth is the main difficulty in observations of such objects. It prevents obtaining pointed images of reference stars and objects of interest simultaneously. The frames for reference stars and objects are obtained separately using the RDS CCD technique. The basic idea of combining the time delay integration (TDI) mode of CCD (Gehrels et al. 1990) with the rotation platform for observations of fast-moving NEAs was presented and discussed by researchers from Shanghai Astronomical Observatory (ShAO) and RI MAO in 2006 (Tang et al. 2006). The basic procedure for utilizing the RDS CCD technique to observe NEOs is described in Tang et al. (2014).

The TDI mode is usually used for imaging long continuous strips of the sky. The exposure time of classical TDI depends only on the speed of a target and field size which cannot be changed (in full exposure time). The implemented RDS CCD technique uses specified exposures during which the CCD camera works in TDI mode (speed of reading out matches the speed of a target and pixel scale). When the specified exposure time is finished, the readout process is started with maximum speed and without the CCD flushing (Shulga et al. 2008).

The CCD with TDI mode is installed on a rotating platform and rotates to make the direction of pixel reading line parallel to the direction of motion for the object. The CCD then works in TDI mode with speed of pixel reading equal to apparent motion of the object. It allows acquiring pointed images of moving objects. Considering the directions of motion, most NEAs are usually close to those of the stars (according to distribution of inclinations to the ecliptic, only 30% of all discovered NEAs have inclination more than 15°). TDI mode can be used also to observe stars but with apparent sidereal velocity ($15 \times \cos(\delta)$) and short exposure time. The pointed images of

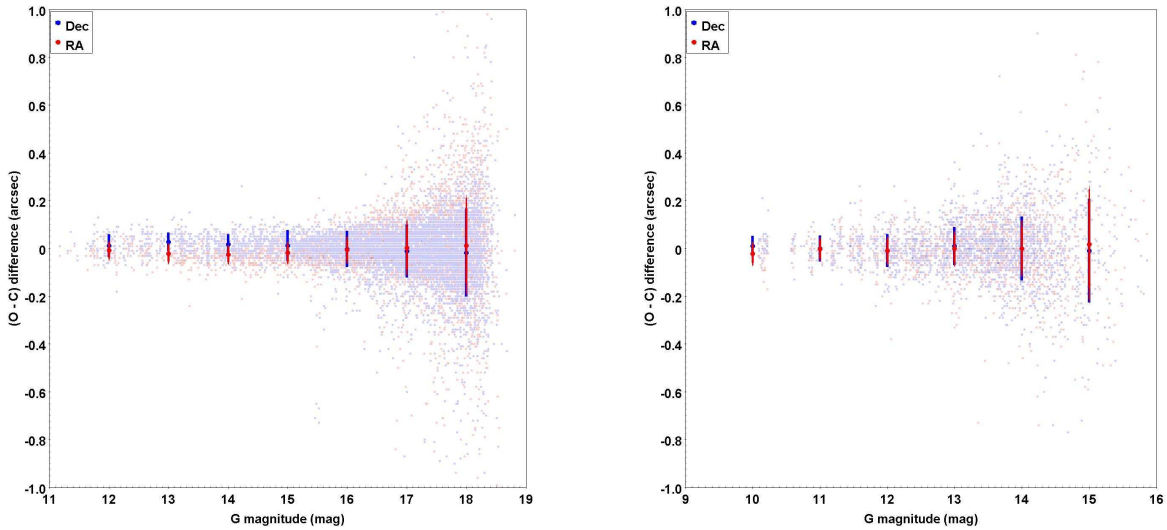

Fig. 2 Mean values of $(O-C)$ differences in reference stars' positions regarding magnitude in the *Gaia* DR2 system with one sigma interval error bars: Lishan telescope, NTSC (*left*); KT-50 telescope, RI MAO (*right*).

stars will be obtained then as reference frames on separate frames from the object. It is necessary to read the lines of the CCD in perfect synchronization with the moving speed of the stars or object on the focal plane of a telescope.

Such observational technique assumes acquiring at least three frames as one set at the fixed telescope position. The telescope and CCD are locked after the telescope is moved to a new target position and the CCD is rotated to the appropriate direction of the apparent motion of the object. First and last frames in the set are referenced with pointed images of stars, while the middle one is taken to get a pointed image of the object. Since the telescope maintains a stable position during one set of observations, the plate constants can be interpolated by a linear function on a short time interval (Kozyryev et al. 2010). Telescope and CCD are moved to a new position after all frames in the set have been taken. An additional requirement is taking observations of objects with hour angles in range $\pm$ 1.5 h around meridian and zenith distances less than 50°, where there are no very large astrometric errors caused by anomalous refraction.

The RDS CCD technique is implemented on two small-sized parallactic optical telescopes. The Lishan telescope is one of them. It belongs to an observational station of NTSC of CAS at Lishan Mountain, near Xi'an city. The first test observations of NEAs were done in October 2018 and regular observations started since the second half of 2019. The IAU MPC observatory code O85 was assigned for Lishan observational station of NTSC of CAS in December 2019. According to an agreement between NTSC and ShAO, part of the observational time belongs to ShAO. The other one is KT-50 which is placed in RI MAO (IAU MPC Observatory code 089). Regular observations of selected asteroids and NEOs at the KT-50 telescope have been conducted since 2011 (Ivantsov et al. 2012). Table 1 gives detailed technical characteristics about the telescopes and instrumental systems. Depending on the exposure time and apparent speed of NEAs, the size of frames is different.

As is known, the accuracy in determining the image center coordinates depends on the signal-to-noise ratio (SNR) and full width at half maximum (FWHM) values (King 1983). The FWHM value does not depend on the brightness of the object and is determined only by the optical design and location of the telescope. With the classical method of observations, in case the object moves at high apparent velocity in the FOV and requires long exposures, its images are stretched. This leads to a deterioration in accuracy when the obtained image is approximated by the point spread function (PSF). The average FWHM for a given telescope can be regarded as an indicator for applying the RDS CCD technique. If the apparent displacement of the object during the supposed exposure exceeds the FWHM value by several times, applying the RDS CCD technique is expedient. Such a threshold value can be defined based on the selected approximation function of the PSF.

The advantage of the RDS CCD technique, especially at the limit of the telescope's capabilities, is the possibility of increasing the exposure time for faint objects, if their speed and direction of motion do not coincide with the diurnal motion of the stars. In this way, application of the RDS CCD technique for observations of such kind objects allows keeping pointed images of them, which yields both a higher SNR value and a possibility of a more accurate

Table 2 NEA Observation Statistics of the RI MAO (code 089) and Lishan Station (code O85)

Year	IAU MPC code	N1	N2	Current year		$(O-C)\pm\sigma\,('')$	
				n1	n2	RA	Dec
2017	089	664	32	246	12	–0.00 ± 0.16	0.06± 0.19
2018	089	915	45	200	12	0.03 ± 0.18	0.09 ± 0.21
2019	089	823	34	121	7	0.02 ± 0.20	0.02 ± 0.23
2019	O85	395	14+4	54	2	–0.01 ± 0.12	0.08 ± 0.13
2020*	089	1108	28	23	4	0.01 ± 0.17	-0.01 ± 0.21
2020*	O85	289	21	12	1	–0.01 ± 0.16	0.04 ± 0.18

* Data regarding November 2020.

image center calculation, and, consequently, the equatorial coordinates.

3 PROCESSING NEA OBSERVATIONS

The processing pipeline for calculation of object's equatorial coordinates includes the next steps:

I) Standard astrometric data reduction of CCD frames with reference stars to calculate equatorial coordinates of optical centers, standard coordinates of reference stars and plate constants;

II) Measurements of the asteroid's rectangular coordinates in the CCD frame;

III) Linear interpolation of obtained plate constants, equatorial coordinates of optical centers at the time associated with frame of the asteroid;

IV) Calculation of the asteroid's equatorial coordinates.

The detailed description of the reduction pipeline algorithm of the combined scheme is given in Sybiryakova et al. (2015).

The first step in processing, related to astrometric reductions of the reference frames, has been carried out by the "Astrometrica" package[4] in automatic mode. No bias, dark or flat-field corrections were applied to the raw CCD frames before processing. According to Evans et al. (2002), the result of applying flat-field corrections in TDI mode of CCD camera is negligible and might be ignored here. Other preprocessing corrections will have even less effect. The FOV of the telescopes and limiting magnitude allow finding a sufficient number of reference stars to perform astrometric data reductions with a 3rd order polynomial for transformations between rectangular and standard coordinates despite the short exposure time (10 – 15 s) for frames with reference stars. The limiting magnitude for the Lishan telescope without optical filters is 18 mag and that for the KT-50 telescope is 16 mag with standard Johnson V filter. The *Gaia* Data Release 2 (DR2) catalog is referenced to perform astrometric data reductions at the present time.

The dependences of the precision of a single observation of the stars in the reference system versus the G magnitude of *Gaia* DR2 system for the telescopes are displayed in Figure 2. The standard deviation of the $(O-C)$ differences of stars' positions is considered as an estimation of the precision, where "O" means observed position and "C" - stars' position from the *Gaia* DR2 catalog. As can be seen from Figure 2, there are no significant deviations from the zero point in $(O-C)$ differences along represented magnitudes. Mean $(O-C)$ values with standard deviation are $-0.01'' \pm 0.08''$ in right ascension and declination for the Lishan telescope and $0.01'' \pm 0.10''$ and $0.01'' \pm 0.09''$ respectively for the KT-50 telescope. There is a noticeable decrease in precision for faint stars, therefore to perform reliable astrometric reductions only the stars in the range 12 – 17.0 mag for Lishan telescope and 11 – 15.0 mag for KT-50 telescope were chosen.

It worth noting that when taking observations of the objects (middle CCD frames of the observational sets with exposures ranging in 25 – 150 s) there are cases when the image of the object crosses the trailed image of a star. Such frames are excluded from processing.

Table 3 2019 JL3 $(O-C)$ Differences (code 089)

Date 2019.05	$(O-C)\,('')$ (1)		$(O-C)\,('')$ (2)	
	RA	Dec	RA	Dec
20.000335	–0.98	0.30	–0.13	–0.06
20.005732	–0.92	0.37	–0.08	0.01
20.011136	–0.80	0.22	0.04	–0.15
20.016528	–0.74	0.33	0.09	–0.00
20.019223	-0.69	0.58	0.14	0.22
20.021921	–1.17	0.28	–0.35	–0.08
20.024617	–0.92	0.55	–0.10	0.17
Mean	**-0.89**	**0.38**	**-0.06**	**0.02**
σ	**0.16**	**0.14**	**0.17**	**0.13**

4 RESULTS AND PRECISION ANALYSIS

The regular observations of asteroids at the Lishan telescope (code O85) using the RDS CCD technique started at the end of 2019. More than 500 observations of 35 NEAs and 4 main belt asteroids (MBAs) were obtained. The MBAs were observed in order to apply for the IAU MPC observatory code. The observations of NEAs at the

[4] Astrometrica, http://www.astrometrica.at

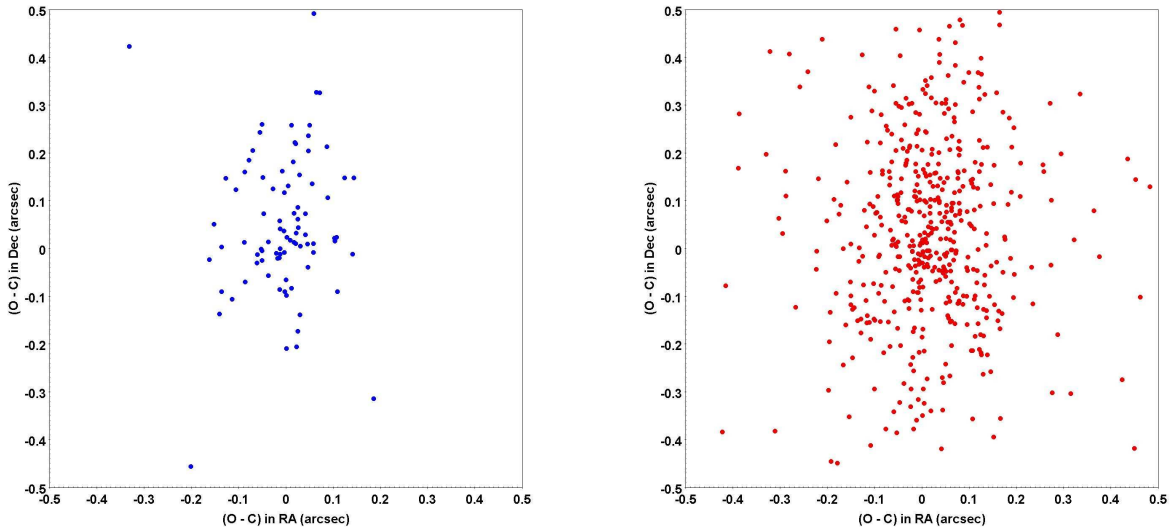

Fig. 3 The mutual distribution of mean $(O - C)$ differences in right ascension and declination for Lishan's (code O85) 2019-2020 observations (*left*) and Mykolaiv's (code 089) 2017–2020 observations (*right*).

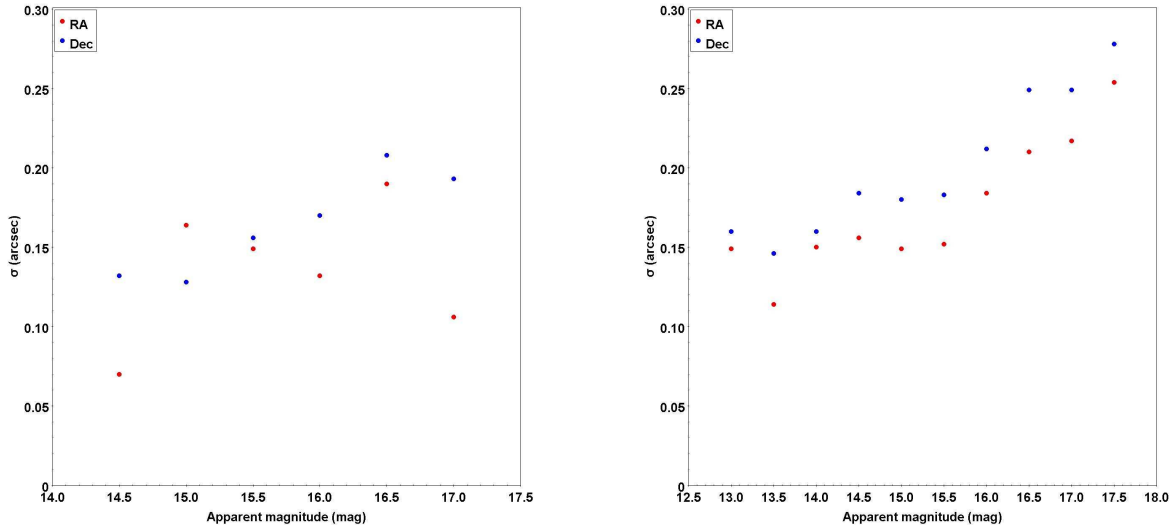

Fig. 4 The averaged standard deviations of the $(O - C)$ differences of a single observational series is plotted against asteroids' apparent magnitude. For the asteroids up to 16 mag these errors are less than $\pm\ 0.2''$, in both coordinates: Lishan's (code O85) (*left*); Mykolaiv's (code 089) (*right*).

Table 4 Results of the Selected PHA Observations

NEA	N1	N2	Uncert. Param.	Min. Dist., * AU		App. Motion, ** $''$ min^{-1}		$(O-C) \pm \sigma$, $''$		Mag
				ephem.	observ.	max.	observ.	RA	Dec	
2019 EA2	22	167	4	0.00205	0.00360	217.21	66.93	0.03 ± 0.25	–0.19 ± 0.39	16.3
2019 JL3	7	60	5	0.00637	0.00649	114.21	105.29	–0.06±0.16	0.01 ± 0.13	16.1
2017 MC4	13	156	2	0.01955	0.02127	87.67	74.61	0.24 ± 0.27	0.00 ± 0.19	16.5
2019 JV1	14	157	6	0.02450	0.03431	59.52	30.79	–0.07 ± 0.25	0.25 ± 0.29	16.5
2019 CD5	6	168	5	0.02597	0.02893	54.25	42.80	0.06 ± 0.14	0.23 ± 0.29	16.5
2018 UQ1	16	254	3	0.02415	0.03718	42.22	17.30	0.12 ± 0.11	0.22 ± 0.13	16.9
2017 YE5	19	346	3	0.03986	0.04060	32.11	30.87	0.07 ± 0.19	–0.03 ± 0.25	16.6
2017 OP68	39	338	4	0.05115	0.05555	18.95	16.14	0.00 ± 0.11	–0.09 ± 0.19	15.6

* Data regarding current apparition observed at RI MAO (089). The column **ephem.** shows possible minimal distance to Earth with respect to Geocenter; the column **observ.** – lists observational site (code 089).
** The column **max.** shows maximum apparent motion with respect to Geocenter; the column **observ.** – regarding observational site (code 089).

KT-50 telescope (code 089) started in 2011 and since then about 8000 positions of more than 400 asteroids were obtained, including more than 3100 positions of 145 PHAs. Unfortunately, weather conditions and the location of the telescope KT-50 significantly restrict the potential and effectiveness of observations. Statistical information on the last 3 years of the NEA observations at Lishan and the KT-50 telescopes is provided in Table 2, where N1, N2 - number of obtained positions and asteroids respectively; n1, n2 - number of positions and asteroids for newly discovered objects in the current year; $(O - C)$ represents the mean residuals between "O" – observed positions and "C" – positions from the NEODyS-2 ephemeris[5] at the time of observations and their standard deviation values, σ.

As can be seen from Table 2, the number of observations obtained by the RDS CCD technique is a small percentage of the growing volume of observations carried out by large monitoring projects such as CSS (with more than 150 000 per year), Pan-STARRS (with more than 300 000 per year) and others (observational statistics[1]). However, it should be noted that most of these positions were obtained in the period of CA to the Earth, when the asteroids moved with high apparent velocities in the FOV and, as a rule, they were observed little by other observers following traditional techniques. Observations of newly discovered (n1, n2) asteroids are especially important in this period in order not to lose them in the next period of visibility. For example, asteroid 2019 JL3 was first observed by the Mt. Lemmon Survey on 2019 May 8[1]. Its CA to the Earth was on 2019 May 20 with minimal distance of 0.006 AU and apparent motion was $105.29''$ min^{-1} (42.12 deg d^{-1}). The last optical observation before the CA moment was obtained on May 12. The total number of observations presented in the IAU MPC database at that time was only 55 positions. RI MAO observations at the KT-50 telescope were performed on 2019 May 20. Comparison of the obtained observations with current JPL's HORIZONS ephemeris has shown large differences, which significantly decreased when these observations were added to the IAU MPC database. Table 3 lists values of the $(O - C)$ differences for the KT-50 observations of 2019 JL3 with JPL's HORIZONS ephemeris, which were calculated on May 20 **(1)** and a few days after this date **(2)**, when the observations were added to the IAU MPC database.

JPL's HORIZONS ephemeris was referenced to get ephemeris positions of the objects for calculation of $(O - C)$ differences. The mutual distribution of all NEA mean $(O - C)$ differences in right ascension and declination is depicted in Figure 3 for Lishan's (code O85) 2019–2020 observations (left) and Mykolaiv's (code 089) 2017–2020 observations (right).

Many of these asteroids have poorly determined orbits and as a result the $(O - C)$ differences can deviate from zero significantly. Therefore, the scatter of these differences (standard deviation) will be a more accurate assessment of the precision of the observations. The standard deviations of the $(O - C)$ differences of single observational series, averaged over bin 0.5 mag, is plotted in Figure 4 versus apparent magnitude.

As can be seen in Figures 3 and 4, precisions of NEAs from Mykolaiv observations are high enough for this kind of object. Mean values of the $(O - C)$ differences with their standard deviation for right ascension and declination are $-0.01'' \pm 0.14''$ and $0.05'' \pm 0.16''$ for the Lishan telescope and $0.02'' \pm 0.18''$ and $0.03'' \pm 0.21''$ for the KT-50 telescope respectively.

As noted in Vereš et al. (2018), a sufficient precision in orbital element determination of newly discovered objects will allow us not to lose them in the next orbital revolution and CA to the Earth. Despite the large number of observational projects, both professional and amateur, application of the RDS CCD technique allows obtaining a significant part of observations of individual objects with sufficient precision. Results of observations for some selected NEAs are displayed in Table 4, where **N1** and **N2** are number of Mykolaiv observations and total amount of observations in the IAU MPC database respectively, **Mag** - means apparent magnitude. **Uncertainty Parameter** is U parameter of IAU MPC which describes quantifying uncertainty in a perturbed orbital solution for the asteroids. Column (5) features the minimal distance to the Earth which a specified NEA has reached in the current CA (**ephem.**) and distance to the Earth where object was observed by RI MAO (**observ.**). The maximum apparent motion at the time of minimal distance to Earth (**max.**) and during observations at RI MAO (**observ.**) are presented in Column (6). Among the presented NEAs, the observations made at RI MAO for 2019 JL3 are last before, and those for 2017 MC4 are first after, CA to Earth in the current orbital revolution.

As can be seen from Table 4, the precision of NEA observations acquired by the RDS CCD technique does not depend on their visible velocity. The RDS CCD technique has the potential in observations of NEAs with high apparent motion in order to reach sufficient precision for regular and follow-up observations because currently a large number of observed NEAs are lost subsequently due to inaccurate orbit determination after CA discovery.

In order to compare results presented in current research with observations of asteroids from around the

[5]NEODyS-2: Near Earth Objects - Dynamic Site, *http://newton.dm.unipi.it/neodys/*

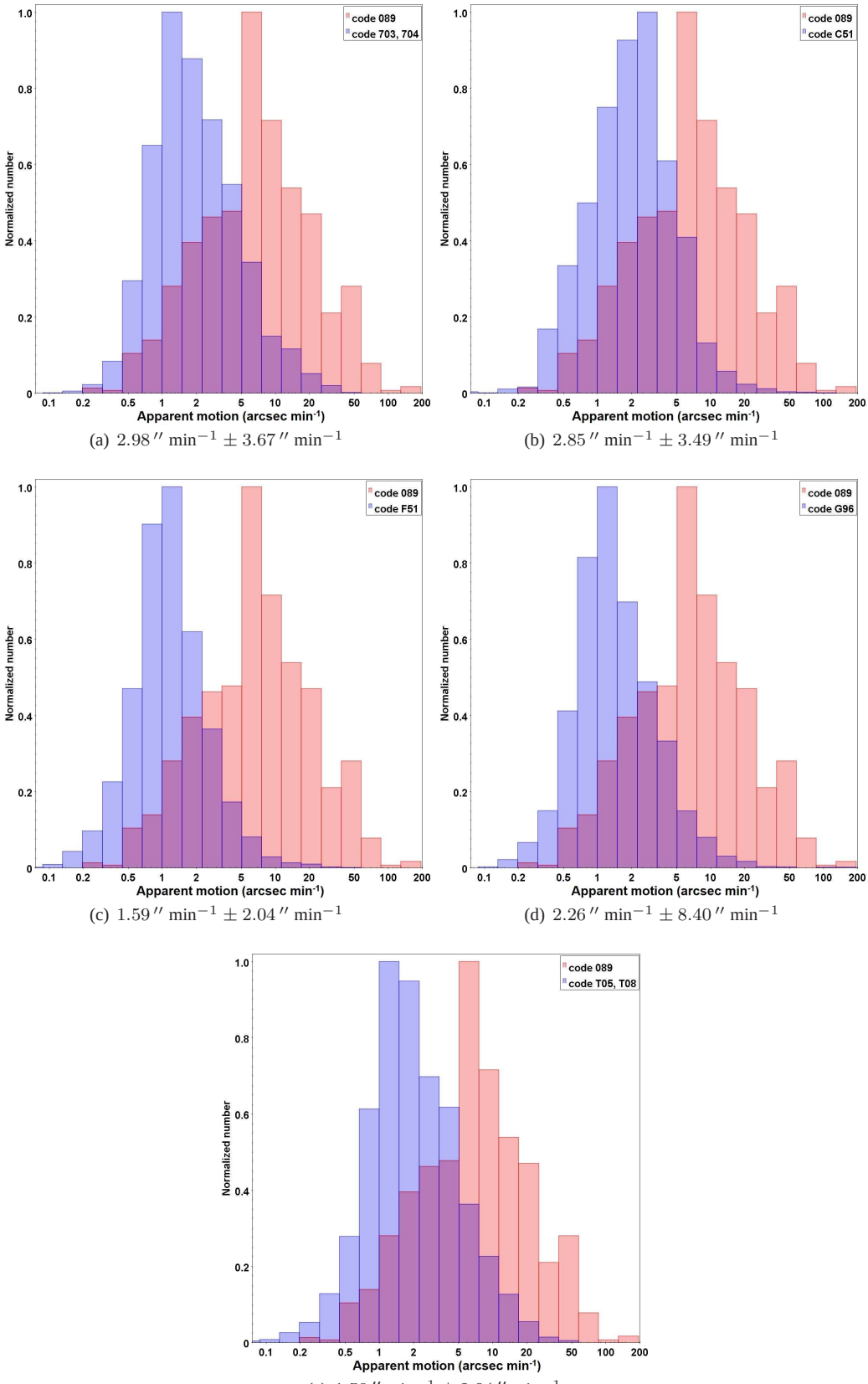

(a) $2.98\,''\ \mathrm{min}^{-1} \pm 3.67\,''\ \mathrm{min}^{-1}$

(b) $2.85\,''\ \mathrm{min}^{-1} \pm 3.49\,''\ \mathrm{min}^{-1}$

(c) $1.59\,''\ \mathrm{min}^{-1} \pm 2.04\,''\ \mathrm{min}^{-1}$

(d) $2.26\,''\ \mathrm{min}^{-1} \pm 8.40\,''\ \mathrm{min}^{-1}$

(e) $1.59\,''\ \mathrm{min}^{-1} \pm 2.04\,''\ \mathrm{min}^{-1}$

Fig. 5 The distribution of apparent motion for NEA observations since 2010 for selected observatories/surveys in comparison to observations of RI MAO (code 089). The mean value of apparent motion and its standard deviation for compared observatory/survey are given in the title of each part; for RI MAO observations, mean and standard deviation are $11.84\,''\ \mathrm{min}^{-1} \pm 14.94\,''\ \mathrm{min}^{-1}$.

Table 5 Averaged Statistics of Observational Precision from the IAU MPC Database Spanning 10 Years

RA (″)		Dec (″)		Observatory IAU MPC code	Observatory name
mean	mean σ	mean	mean σ		
0.00	0.25	0.04	0.26	089	RI MAO
0.06	0.65	0.30	0.62	703, 704	Catalina Sky Survey
0.05	0.54	0.02	0.59	C51	WISE (NEOWISE)
0.03	0.13	0.07	0.14	F51	Pan-STARRS 1
0.02	0.32	0.05	0.29	G96	Mt. Lemmon Survey
0.02	0.47	0.08	0.49	T05, T08	ATLAS-HKO, ATLAS-MLO
0.01	0.48	0.03	0.45	All observatories	

world, an analysis of statistical information presented on the IAU MPC website regarding precision of asteroid observations has been done. The observatories or surveys mentioned in Section 1 including RI MAO were chosen for analysis. Only data since 2010 have been analyzed. Unfortunately, the IAU MPC service stopped providing such statistical data in 2018, so there are no data for the Lishan telescope. Table 5 displays averaged $(O - C)$ differences in right ascension and declination ("mean") with averaged standard deviation values ("mean σ") presented in residual information of IAU MPC[1] for selected surveys for the considered time period.

The precision of observations of RI MAO is higher than average for "all observatories" and at the same level with considered observatories/surveys despite the apparent motion of objects in these observations being higher. Figure 5 features the distribution of apparent speed for mentioned observatories/surveys among the NEA observations since 2010. The presented comparison demonstrates, in general, observations obtained at the KT-50 telescope of RI MAO (code 089) that were taken when observed NEAs had higher apparent motion.

It should be noted that the comparison of apparent speed distributions of big surveys with our RDS observations might seem, to some measure, incorrect from the point of view of the difference in the required tasks. The main tasks of the surveys are monitoring all known asteroids and discovering new ones. The described RDS CCD technique is mainly applicable for targeted observations of fast-moving objects due to the specifics of the observational process based on the apparent motion of the object. The purpose of the provided comparison is to demonstrate that observations utilizing the RDS CCD technique have precision at a comparable level with the best ground-based optical observations of NEAs.

The usage of the RDS CCD technique gives the opportunity to observe the approaching object at minimal distance to the Earth during high apparent speed. Part of observations carried out in RI MAO in 2017 utilizing the RDS CCD technique have index "**h**" (high precision) according MPC statistics (observational statistics[1]) which indicate reliability of obtained observations and employed observational technique.

5 CONCLUSIONS

This paper describes the RDS CCD technique for observations of fast moving PHAs during their CA to the Earth. The technique was implemented on two small-sized parallactic optical telescopes: Lishan telescope of NTSC since 2018 and RI MAO KT-50 telescope since 2011. The results of processing the observations obtained using this technique confirm that the precision of the positions with respect to JPL's HORIZONS ephemeris system is in the range $0.1'' - 0.3''$ for the asteroids with apparent magnitudes up to 17 mag. In order to estimate the external precision of presented observations and compare them with the data of other observatories, the IAU MPC statistical results for all observatories over 2010 - 2018 have been used. The analysis of statistics from the IAU MPC database shows that this is a good level of precision for observations of such objects. In addition, the ability to obtain pointed images of fast asteroids at moments of CA to the Earth expands the orbit arc, which can be useful for refining the orbital elements and not lose this object in the next period of visibility. It is expected that decreasing average size of newly discovered NEAs in the future will lead to detection at closer distance to the Earth with higher apparent motion and the RDS CCD technique has the potential to acquire observations of such objects with sufficient precision.

Acknowledgements This research is supported by the National Natural Science Foundation of China (Grant Nos. U1831133 and 12073062) and National Astronomical Data Center of China.

References

Evans, D. W., Irwin, M. J., & Helmer, L. 2002, A&A, 395, 347
Gehrels, T., McMillan, R. S., Scotti, J. V., & Perry, M. L. 1990, in Astronomical Society of the Pacific Conference Series, 8, CCDs in astronomy, ed. G. H. Jacoby, 51
Harris, A. W., & D'Abramo, G. 2015, Icarus, 257, 302

Ivantsov, A., Pomazan, A., Kryuchkovskiy, V., & Gudkova, L. 2012, Odessa Astronomical Publications, 25, 66
Jedicke, R., Granvik, M., Micheli, M., et al. 2015, Surveys, Astrometric Follow-Up, and Population Statistics, Asteroids IV (University of Arizona Press, Tucson), 795
Jones, R. L., Slater, C. T., Moeyens, J., et al. 2018, Icarus, 303, 181
King, I. R. 1983, PASP, 95, 163
Kozyryev, Y. S., Sybiryakova, Y. S., & Shulga, A. V. 2010, Kosm. Nauka Tehnology, 16, 71
Larson, S., Brownlee, J., Hergenrother, C., & Spahr, T. 1998, in Bulletin of the American Astronomical Society, Vol. 30, 1037
Maigurova, N. V., Pomazan, A. V., & Shulga, A. V. 2018, Odessa Astronomical Publications, 30, 216
Mainzer, A., Bauer, J., Cutri, R. M., et al. 2014, ApJ, 792, 30
Shulga, O., Kozyryev, Y., & Sibiryakova, Y. 2008, in A Giant Step: from Milli- to Micro-arcsecond Astrometry, eds. W. J. Jin, I. Platais, & M. A. C. Perryman, 248, 128
Sybiryakova, Y. S., Shulga, O. V., Vovk, V. S., Kulichenko, M. O., & Kozyryev, Y. S. 2015, Kinematics and Physics of Celestial Bodies, 31, 296
Tang, Z. H., Pinigin, G., & Shulga, A. V. 2006, in Proc. of the Intern. Sc. Conf., Enlargement of Collaboration in Ground-Based Astronomical Research in SEE Countries, Studies of the Near-Earth and Small Bodies of the Solar System., eds. G. Pinigin et al. (Mykolaiv: Atoll), 184, http://www.nao.nikolaev.ua/articles/nao185/2006_Tang_a_15.pdf
Tang, Z.-H., Mao, Y.-D., Li, Y., et al. 2014, Mem. Soc. Astron. Italiana, 85, 821
Tonry, J. L., Denneau, L., Heinze, A. N., et al. 2018, PASP, 130, 064505
Tricarico, P. 2017, Icarus, 284, 416
Trilling, D. E., Valdes, F., Allen, L., et al. 2017, AJ, 154, 170
Vereš, P., Payne, M. J., Holman, M. J., et al. 2018, AJ, 156, 5
Wainscoat, R. J., Weryk, R., & Chambers, K. 2018, in American Astronomical Society Meeting Abstracts, 231, 115.05